Light-scattering detection of quantum phases of ultracold atoms in optical lattices

Jinwu Ye, J. M. Zhang, W. M. Liu, Keye Zhang, Yan Li, and Weiping Zhang

Light scattering detection of quantum phases of ultracold atoms in optical lattices

Jinwu Ye [1,2], J.M. Zhang [3], W.M. Liu [3], Keye Zhang [4], Yan Li[4] and Weiping Zhang [4]

[1] *Department of Physics, Capital Normal University, Beijing, 100048 China*
[2] *Department of Physics, The Pennsylvania State University, University Park, PA, 16802, USA*
[3] *Institute of Physics, Chinese Academy of Sciences, Beijing, 100080, China*
[4] *Department of Physics, East China Normal university, Shanghai, 200062, China*

Ultracold atoms loaded on optical lattices can provide unprecedented experimental systems for the quantum simulations and manipulations of many quantum phases. However, so far, how to detect these quantum phases effectively remains an outstanding challenge. Here, we show that the optical Bragg scattering of cold atoms loaded on optical lattices can be used to detect many quantum phases which include not only the conventional superfluid and Mott insulating phases, but also other important phases such as various kinds of density waves (CDW), valence bond solids (VBS), CDW supersolids and VBS supersolids.

Various kinds of strongly correlated quantum phases of matter may have wide applications in quantum information processing, storage and communications [1]. It was widely believed and also partially established that due to the tremendous tunability of all the parameters in this system, ultracold atoms loaded on optical lattices (OL) can provide an unprecedented experimental systems for the quantum simulations and manipulations of these quantum phases and quantum phase transitions between these phases. For example, Mott and superfluid phases [2] may have been successfully simulated and manipulated by ultra-cold atoms loaded in a cubic optical lattice [3]. However, there are still at least two outstanding problems remaining. The first is how to realize many important quantum phases [1]. The second is that assuming the favorable conditions to realize these quantum phases are indeed achieved in experiments, how to detect them without ambiguity. In this paper, we will focus on the second question. So far the experimental way to detect these quantum phases is mainly through the time of flight (TOF) measurement [1, 3] which simply opens the trap and turn off the optical lattice and let the trapped atoms expand and interfere, then take the image. The atom Bragg spectroscopy is based on stimulated matter waves scattering by *two* incident laser pulses [4, 5] through the TOF measurements. The momentum [4] transfer Bragg spectroscopy was used to detect the Bogoliubov mode inside an BEC condensate. The energy transfer [5] Bragg spectroscopy was used to detect the Mott gap in a Mott state in an optical lattice. Optical Bragg scattering (Fig.1) has been used previously to study periodic lattice structures of cold atoms loaded on optical lattices [6]. It was also proposed as an effective method for the thermometry of fermions in an optical lattice [7] and to detect putative anti-ferromagnetic (AF) ground state of fermions in OL [8]. There are very recent optical Bragg scattering experimental data from a Mott state, a BEC and AF state [9]. The atom Bragg spectroscopy and Optical Bragg scattering are two different, but complementary experimental methods.

In this paper, we will develop a systematic theory of using the optical Bragg scattering (Fig.1) to detect the nature of quantum phases of interacting bosons loaded in optical lattices. We show that the optical Bragg scattering not only couples to the density order parameter, but also the *valence bond order* parameter due to the hopping of the bosons on the lattice. At integer fillings, when $\vec{q}$ matches a reciprocal lattice vector $\vec{K}$ of the underlying OL, there is an increase in the optical scattering cross section as the system evolves from the Mott to the SF state due to the increase of hopping in the SF state. At 1/2 filling, in the CDW state, when $\vec{q}$ matches the CDW ordering wavevector $\vec{Q}_n$ and $\vec{K}$, there is a diffraction peak proportional to the CDW order parameter squared and the density squared respectively (Fig.3a), the ratio of the two peaks is a good measure of the CDW order parameter. In the VBS state, when $\vec{q}$ matches the VBS ordering wavevector $\vec{Q}_K$, there is a much smaller, but detectable diffraction peak proportional to the VBS order parameter squared, when it matches $\vec{K}$, there is also a diffraction peak proportional to the uniform density in the VBS state (Fig.3b). All the diffraction peaks scale as the square of the numbers of atoms inside the trap. All these characteristics can determine uniquely CDW and VBS state at 1/2 filling and the corresponding CDW supersolid and VBS supersolid slightly away from the 1/2 filling. In the following, we just take 2d optical lattices as examples. The 1d and 3d cases can be similarly discussed.

The Extended Boson Hubbard Model (EBHM) with various kinds of interactions, on all kinds of lattices and at different filling factors is described by the following Hamiltonian [2, 10–17]:

$$H_{BH} = -t \sum_{\langle ij \rangle} (b_i^\dagger b_j + h.c.) - \mu \sum_i n_i + \frac{U}{2} \sum_i n_i(n_i - 1)$$
$$+ V_1 \sum_{<ij>} n_i n_j + V_2 \sum_{\langle ik \rangle} n_i n_k + \cdots \qquad (1)$$

where $n_i = b_i^\dagger b_i$ is the boson density, t is the nearest neighbor hopping which can be tuned by the depth of the optical lattice potential, the U, V_1, V_2 are onsite, nearest neighbor (nn) and next nearest neighbor (nnn) interactions respectively, the $\cdots$ may include further neighbor
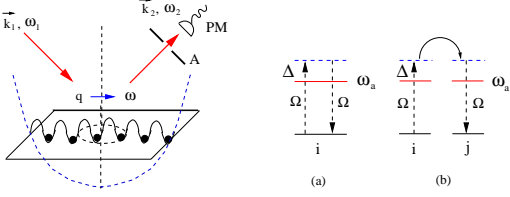
FIG. 1: Optical Bragg scattering of cold atoms moving in 2 dimensional optical lattices. The $\vec{q} = \vec{k}_1 - \vec{k}_2$ and $\omega = \omega_1 - \omega_2$ are momentum and energy transfer from the laser beams to the cold atoms respectively. The A stands for a aperture, the PM stands for a Photomultiplier. The off resonant scattering processes lead to the on-site term (a) and the off-site term (b) in Eqn.3.
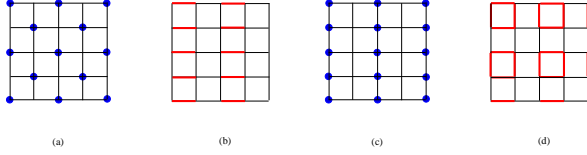

FIG. 2: The charge density wave (CDW) phase in a square lattice at $n_0 = 1/2$ with ordering wavevector $\vec{Q}_n = (\pi, \pi)$. (b) valence bond solid (VBS) phases with ordering wavevector $\vec{Q}_K = (\pi, 0)$ where the kinetic energy $\langle K_{ij} \rangle = \langle b_i^\dagger b_j + h.c. \rangle$ takes a non-zero constant K in the two sites connected with a dimer, but 0 in the two sites without a dimer. (c) Stripe CDW order at $\vec{Q}_n = (\pi, 0)$ and (d) Plaquette VBS order at $\vec{Q}_n = (\pi, 0), (0, \pi)$. [2, 10–17].

interactions and possible ring-exchange interactions. The filling factor $n = N_a/N$ where N_a is the number of atoms and N is the number of lattice sites. The on-site inter-action U can be tuned by the Feshbach resonance [2]. Various kinds of optical lattices such as honeycomb, tri-angular [18], body-centered-cubic [18], Kagome lattices [19] can be realized by suitably choosing the geometry of the laser beams forming the optical lattices. There are many possible ways to generate longer range interac-tion $V_1, V_2, ...$ of ultra-cold atoms loaded in optical lat-tices. Being magnetically or electrically polarized, the ^{52}Cr atoms [20] or polar molecules [21] $^{40}K +^{87} Rb$ (or $^{39}K +^{87} Rb$) interact with each other via long-rang anisotropic dipole-dipole interactions. Loading the ^{52}Cr or the polar molecules on a 2d optical lattice with the dipole moments perpendicular to the trapping plane can be mapped to Eqn.1 with long-range repulsive interac-tions $\sim p^2/r^3$ where p is the dipole moment. The CDW supersolid phases studied by QMC [11] and described in [15] by the dual vortex method was numerically found to be stable in large parameter regimes in this system [22]. The generation of the ring exchange interaction has been discussed in [24]. Some of the important phases with long range interactions are listed in Fig.2. Recently, the quantum entanglement properties of the VB state was addressed in [25].

The interaction between the two laser beams in Fig.1

with the two level bosonic atoms is:

$$
\begin{aligned}
H_{int} = & \int d^2\vec{r}\Psi^\dagger(\vec{r})[\frac{\vec{p}^2}{2m_a} + V_{OL}(\vec{r}) + \frac{\hbar\omega_a}{2}\sigma_z \\
& + \frac{\Omega}{2}\sum_l (e^{-i\omega_l t}\sigma^+ u_l(\vec{r}) + h.c.)]\Psi(\vec{r}) \quad (2)
\end{aligned}
$$

where $\Psi(\vec{r}) = (\psi_e, \psi_g)$ is the two component boson an-nihilation operator, the incident and scattered lights in Fig.1a and the two incident lights in Fig.1b have frequen-cies ω_l and mode functions $u_l(\vec{r}) = e^{i\vec{k}_l \cdot \vec{r} + i\phi_l}$. The Rabi frequencies Ω are much weaker than the laser beams (not shown in Fig.1) which form the optical lattices. When it is far off the resonance, the laser light-atom detunings $\Delta_l = \omega_l - \omega_a$ where ω_a is the two level energy differ-ence are much larger than the Rabi frequency Ω and the energy transfer $\omega = \omega_1 - \omega_2$ (See Fig.1a and 1b), so $\Delta_1 \sim \Delta_2 = \Delta$. After adiabatically eliminating the up-per level e of the two level atoms, expanding the ground state atom field operator $\psi_g(\vec{r}) = \sum_i b_i w(\vec{r} - \vec{r}_i)$ in Eqn.2 where $w(\vec{r} - \vec{r}_i)$ is the localized Wannier functions of the lowest Bloch band corresponding to $V_{OL}(\vec{r})$ and b_i is the annihilation operator of an atom at the site i in the Eqn.1, then we get the effective interaction between the off-resonant laser beams and the ground level g:

$$
H_{int} = \hbar\frac{\Omega^2}{\Delta}e^{-i\omega t}[\sum_i^N J_{i,i}n_i + \sum_{<ij>}^N J_{i,j}b_i^\dagger b_j] \quad (3)
$$

where the interacting matrix element is $J_{i,j} = \int d\vec{r}w(\vec{r} - \vec{r}_i)u_1^*(\vec{r})u_2(\vec{r})w(\vec{r} - \vec{r}_j) = J_{j,i}$. The first term in Eqn.3 is the on-site term $\hat{D} = \sum_i^N J_{i,i}n_i$ (See Fig.1a). The second term is the off-site term (See Fig.1b). Because the Wannier wavefunction $w(\vec{r})$ can be taken as real in the lowest Bloch band, the off-site term can be written as $\hat{K} = \sum_{<ij>}^N J_{i,j}b_i^\dagger b_j = \sum_{<ij>}^N J_{i,j}(b_i^\dagger b_j + h.c.)$ which is nothing but the off-site coupling to the nearest neighbor kinetic energy of the bosons $K_{ij} = b_i^\dagger b_j + h.c.$.

It is easy to show that:

$$
\hat{D}(\vec{q}) = f_0(\vec{q})\sum_{i=1}^N e^{-i\vec{q}\cdot\vec{r}_i}n_i = Nf_0(\vec{q})n(\vec{q}) \quad (4)
$$

where $\vec{q} = \vec{k}_1 - \vec{k}_2$, $f_0(\vec{q}) = \int d\vec{r}e^{-i\vec{q}\cdot\vec{r}}w^2(\vec{r})$ and $n(\vec{q}) = \frac{1}{N}\sum_{i=1}^N e^{-i\vec{q}\cdot\vec{r}_i}n_i = \sum_{\vec{k}} b_{\vec{k}}^\dagger b_{\vec{k}+\vec{q}}$ is the Fourier transform of the density operator at the momentum $\vec{q}$. Note that $n(\vec{q}) = n(\vec{q} + \vec{K})$. The wavevector is confined to $L^{-1} < q < a^{-1}$ where the trap size $L \sim 100\mu m$ and the lattice constant $a \sim 0.5\mu m$ in Fig.1. In fact, more information is encoded in the off-site kinetic coupling in Eqn.3. In a square lattice, the bonds are either oriented along the $\hat{x}$ axis $\vec{r}_j - \vec{r}_i = \hat{x}$ or along the $\hat{y}$ axis $\vec{r}_j - \vec{r}_i = \hat{y}$, we have:

$$
\hat{K}_\square = N[f_x(\vec{q})K_x(\vec{q}) + f_y(\vec{q})K_y(\vec{q})] \quad (5)
$$

where $K_\alpha(\vec{q}) = \frac{1}{N}\sum_{i=1}^N e^{-i\vec{q}\cdot\vec{r}_i}K_{i,i+\alpha} = e^{iq_\alpha/2}\sum_{\vec{k}}\cos k_\alpha b_{\vec{k}}^\dagger b_{\vec{k}+\vec{q}}$ are the Fourier transform of the

kinetic energy operator $K_{ij} = b_i^\dagger b_j + h.c.$ along $\alpha = x, y$ bonds at the momentum $\vec{q}$ and the "form" factors $f_\alpha(\vec{q}) = f(\vec{q}, \vec{r}_i - \vec{r}_j = \alpha) = \int d\vec{r} e^{-i\vec{q}\cdot\vec{r}} w(\vec{r}) w(\vec{r} + \vec{r}_i - \vec{r}_j)$. Note that $K_\alpha(\vec{q}) = K_\alpha(\vec{q} + \vec{K})$. Following the harmonic approximation used in [2], we can estimate that $f_0(\pi, 0) \sim e^{-\frac{1}{4}(V_0/E_r)^{-1/2}}$, $f_x(\pi, 0) \sim ie^{-\frac{1}{4}(V_0/E_r)^{-1/2} - \frac{\pi^2}{4}(V_0/E_r)^{1/2}}$, so $|f_x(\pi, 0)/f_0(\pi, 0)| \sim e^{-\frac{\pi^2}{4}\sqrt{V_0/E_r}}$ where V_0 and $E_r = \hbar^2 k^2/2m$ are the strength of the optical lattice potential and the recoil energy respectively [2]. The $f_0(\pi, 0)$ is close to 1 when $V_0/E_r > 4$. It is instructive to relate this ratio to that of the hopping t over the onsite interaction U in the Eqn.1: $|f_x(\pi, 0)/f_0(\pi, 0)| \sim \frac{t}{U}\frac{a_s}{a}$ where a_s is the zero field scattering length and $a = \lambda/2 = \pi/k$ is the lattice constant, using the typical values $t/U \sim 10^{-1}, a_s/a \sim 10^{-2}$, one can estimate $|f_\alpha/f_0| \sim 10^{-3}$. Note that the harmonic approximation works well only in a very deep optical lattice $V_0 \gg E_r$, so the above value *underestimates* the ratio, so we expect $|f_\alpha/f_0| \geq 10^{-3}$.

The differential scattering cross section of the light from the cold atom systems in the Fig.1 can be calculated by using the standard linear response theory:

$$\frac{d\sigma}{d\Omega dE} = \mathcal{S}(\vec{q}, \omega) \sim (\frac{\Omega^2}{\Delta})^2 N^2 [|f_0(\vec{q})|^2 S_n(\vec{q}, \omega) + \sum_{\alpha=\hat{x},\hat{y}} |f_\alpha(\vec{q})|^2 S_{K_\alpha}(\vec{q}, \omega)] \quad (6)$$

where $\vec{q} = \vec{k}_1 - \vec{k}_0, \omega = \omega_1 - \omega_2$, the $S_n(\vec{q}, \omega) = \langle n(-\vec{q}, -\omega)n(\vec{q}, \omega) \rangle$ is the dynamic density-density response function whose Lehmann representation was listed in [4]. The $S_{K_\alpha}(\vec{q}, \omega) = \langle K_\alpha(-\vec{q}, -\omega)K_\alpha(\vec{q}, \omega) \rangle$ is the bond-bond response function whose Lehmann representation can be got from that of the $S_n(\vec{q}, \omega)$ simply by replacing the density operator $n(\vec{q})$ by the bond operator $K_\alpha(\vec{q})$. The integrated scattering cross section over the final energy $\frac{d\sigma}{d\Omega} = \int dE \frac{d\sigma}{d\Omega dE}$ is proportional to the *equal-time* response function $\frac{d\sigma}{d\Omega} = \mathcal{S}(\vec{q}) \sim (\frac{\Omega^2}{\Delta})^2 N^2 [|f_0(\vec{q})|^2 S_n(\vec{q}) + \sum_{\alpha=\hat{x},\hat{y}} |f_\alpha(\vec{q})|^2 S_{K_\alpha}(\vec{q})]$.

We first look at the superfluid to Mott transition at integer filling factor n. When $\vec{q}$ is equal to the shortest reciprocal lattice vector $\vec{K} = (2\pi, 0)$, in the Mott state, $\frac{d\sigma^M}{d\Omega} \sim |f_0^M(2\pi, 0)|^2 N^2 n^2$, in the superfluid state, $\frac{d\sigma^{SF}}{d\Omega} \sim |f_0^{SF}(2\pi, 0)|^2 N^2 n^2 + 2|f_x^{SF}(2\pi, 0)|^2 N^2 B^2$ where B is the average kinetic energy on a bond in the superfluid side. Because $|f_0^{SF}(2\pi, 0)|^2 \sim |f_0^M(2\pi, 0)|^2 \sim 1$ and B is appreciable in the superfluid side, we expect a dramatic increase of the scattering cross section

$$\frac{d\sigma^{SF}}{d\Omega} - \frac{d\sigma^M}{d\Omega} = 2|f_x^{SF}(2\pi, 0)|^2 N^2 B^2 \quad (7)$$

across the Mott to the SF transition due to the prefactor N^2. This prediction could be tested immediately. Surprisingly, there is no such optical Bragg scattering experiment in the superfluid yet.

In the CDW with $\vec{Q}_n = (\pi, \pi)$ in Fig.2a, due to the lack of VBS order on both sides, the second term in Eqn.6 can be neglected, so that

$$\frac{d\sigma}{d\Omega dE}|_{CDW} \sim (\frac{\Omega^2}{\Delta})^2 N^2 |f_0(\vec{q})|^2 S_N(\vec{q}, \omega) \quad (8)$$

which should show a peak at $\vec{q} = \vec{Q}_n$ (Fig.3a) whose amplitude scales as the *square* of the number of atoms inside the trap $\sim |f_0(\pi, \pi)|^2 N^2 m^2$ where $m = n_A - n_B$ is the CDW order parameter [15]. When $\vec{q} = \vec{K}$, then $\mathcal{S}_{CDW}(\vec{K}) \sim |f_0(2\pi, 0)|^2 N^2 n^2$ where $f_0(2\pi, 0) \sim f_0^2(\pi, \pi)$ (Fig.3a). So the ratio of the two peaks in Fig.3a is $\sim m^2/n^2$ if one neglects the very small difference of the two form factors. Slightly away from 1/2 filling, the CDW in Fig.2a may turn into the CDW supersolid (CDW-SS) phase through a second order phase transition [15]. Then we have $\langle n(\vec{q}) \rangle = m\delta_{\vec{q}, \vec{Q}_n} + n\delta_{\vec{q}, 0}$ where $n = n_A + n_B = 1/2 + \delta n$. The superfluid density $\rho_s \sim \delta n = n - 1/2$. The scattering cross section inside the CDW-SS: $\mathcal{S}_{CDW-SS}(\vec{Q}_n) \sim |f_0(\pi, \pi)|^2 N^2 m^2$ stays more or less the same as that inside the CDW, but $\mathcal{S}_{CDW-SS}(\vec{K}) \sim |f_0(2\pi, 0)|^2 N^2 n^2 + 2|f_x(2\pi, 0)|^2 N^2 (\delta n)^2 B^2$ will increase. The B is the average bond strength due to very small superfluid component $\rho_s \sim \delta n = n - 1/2$ flowing through the whole lattice. So the right peak in Fig.3a will increase due to the increase of the total density and the superfluid component inside the CDW-SS phase.

Now we discuss the VBS state with $\vec{Q}_K = (\pi, 0)$ in Fig.2b. Due to the *uniform* distribution of the density in the VBS, when $\vec{q} = \vec{K}$, the second term in Eqn.6 can be neglected, so there is a diffraction peak (Fig.3b) whose amplitude scales as the *square* of the number of atoms inside the trap $\sim |f_0(2\pi, 0)|^2 N^2 n^2$ where $f_0(2\pi, 0) \sim f_0^4(\pi, 0)$ and $n = 1/2$ is the uniform density in the VBS state. However, when one tunes $\vec{q}$ near $\vec{Q}_K$, the first term in Eqn.6 can be neglected, then

$$\frac{d\sigma}{d\Omega dE}|_{VBS} \sim (\frac{\Omega^2}{\Delta})^2 N^2 \sum_{\alpha=\hat{x},\hat{y}} |f_\alpha(\vec{q})|^2 S_{K_\alpha}(\vec{q}, \omega) \quad (9)$$

which should show a peak at $\vec{q} = \vec{Q}_K$ signifying the VBS ordering at $\vec{Q}_K$ whose amplitude scales also as the *square* of the number of atoms inside the trap $\sim |f_x(\pi, 0)|^2 N^2 K^2$ where $K = K_x - K_y$ is the VBS order parameter [15]. So the ratio of the VBS peak at $\vec{q} = \vec{Q}_K$ over the uniform density peak at $\vec{q} = \vec{K}$ is $\sim K^2/n^2 |f_x(\pi, 0)/f_0(2\pi, 0)|^2 \geq 10^{-5}$. However, the smallness of $|f_x|^2$ is compensated by the large number of atoms $N \sim 10^6$, $|f_x|^2 N^2 = (|f_x|^2 N) \times N \sim N \sim 10^6$. Therefore, the Bragg scattering cross section from the VBS order is $\geq 10^{-5}$ smaller than that at $\vec{q} = \vec{K}$ at the same incident energy I_{in} (Fig.3b), but still $\sim 10^6$ above the background, so very much visible in the current optical Bragg scattering experiments. Slightly away from 1/2 filling, the VBS may turn into VB Supersolid (VB-SS) through a second order transition [15]. We have
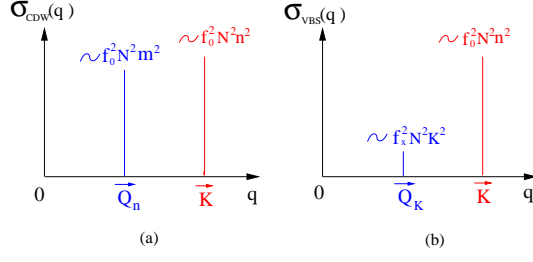
FIG. 3: The optical scattering cross section in (a) CDW, the ratio of the peak at $\vec{Q}_n$ over that at $\vec{K}$ is $\sim m^2/n^2 \sim 1$. (b) VBS state, the ratio of the peak at $\vec{Q}_K$ over that at $\vec{K}$ is $\sim |f_x/f_0|^2 K^2/n^2 \geq 10^{-5}$, but still should be visible in the current optical Bragg scattering experiments.

$\langle K_x(\vec{q}) \rangle = B\delta_{\vec{q},0} + K\delta_{\vec{q},\vec{Q}_K}$ and $\langle n(\vec{q}) \rangle = (\delta n + 1/2)\delta_{\vec{q},0}$. The superfluid density $\rho_s \sim \delta n = n - 1/2$. The scattering cross section inside VB-SS: $\mathcal{S}_{VB-SS}(\vec{Q}_K) \sim |f_x(\pi,0)|^2 N^2 K^2$ stays more or less the same as that inside the VBS, but $\mathcal{S}_{VB-SS}(\vec{K}) \sim |f_0(2\pi,0)|^2 N^2 n^2 + |f_x(2\pi,0)|^2 N^2(\delta n)^2 B_x^2 + |f_y(2\pi,0)|^2 N^2(\delta n)^2 B_y^2$ where $n = 1/2 + \delta n$ and the B_x, B_y are the average bond strengths along x and y due to very small superfluid component $\rho_s \sim \delta n = n - 1/2$ flowing through the whole lattice. So the right peak in Fig.3b will increase due to

the increase of the total density and the superfluid component inside the VB-SS phase. Very similarly, one can discuss the VBS order at $\vec{q} = \vec{Q}_K = (0, \pi)$. For the plaquette VBS order in Fig.2d, then one should be able to see the $S_K(\vec{q})$ peaks at both $(\pi, 0)$ and $(0, \pi)$. So the dimer VBS and the plaquette VBS can also be distinguished by the optical Bragg scattering.

In this paper, we only focused on the optical Bragg scattering detections of the various ground states in a square lattice. The detections of the excitation spectra, the generalization to frustrated lattices, the effects of finite temperature and a harmonic trap will be discussed in a future publication.

[1] For a review, see M. Lewenstein, *et. al.*, Adv. Phys. 56, 243-379 (2007); I. Bloch, J. Dalibard, W. Zwerger, Rev. Mod. Phys. 80, 885 (2008).

[2] D. Jaksch, C. Bruder, J. I. Cirac, C. W. Gardiner, and P. Zoller, Phys. Rev. Lett. 81, 3108 - 3111 (1998).

[3] M. Greiner, *et. al.*, Nature 415, 39-44 (2002).

[4] M. Kozuma, *et al.*, Phys. Rev. Lett. 82, 871 (1999); J. Stenger *et al.*, Phys. Rev. Lett. 82, 4569 (1999); D. M. Stamper-Kurn *et al.*, Phys. Rev. Lett. 83, 2876 - 2879 (1999); J. Steinhauer, *et al.*, Phys. Rev. Lett. 88, 120407, (2002); S. B. Papp, *et al.*, Phys. Rev. Lett. 101, 135301 (2008); P. T. Ernst, *et al.*, Nature Physics 6, 56 (2010).

[5] T. Stoferle *et al.*, Phys. Rev. Lett. 92, 130403 (2004).

[6] G. Birkl, *et al.*, Phys. Rev. Lett. 75, 2823 (1995); M. Weidemuller, *et al.*, Phys. Rev. Lett. 75, 4583 (1995), Phys. Rev. A 58, 4647 (1998).

[7] J. Ruostekoski, C. J. Foot, and A. B. Deb, Phys. Rev. Lett. 103, 170404 (2009).

[8] T. A. Corcovilos *et al.*, Phys. Rev. A 81, 013415 (2010).

[9] I. Bloch, private communication.

[10] G. Murthy, D. Arovas, A. Auerbach , Phys. Rev. B 55, 3104-3121 (1997).

[11] F. Hebert *et al.*, Phys. Rev. B 65, 014513 (2001), P. Sengupta, *et al.*, Phys. Rev. Lett. 94, 207202 (2005);

[12] S. V. Isakov, *et al.*, Phys. Rev. Lett. 97, 147202 (2006); Kedar Damle, T. Senthil, Phys. Rev. Lett. 97, 067202 (2006).

[13] Balents L, *et al.*, Phy. Rev. B 71, 144508 (2005).

[14] Longhua Jiang and Jinwu Ye, J. Phys, Condensed Matter. 18 (2006) 6907-6922

[15] Jinwu Ye, cond-mat/0503113, Nucl. Phys. B 805 (3) 418-440 (2008).

[16] Yan Chen and Jinwu Ye, updated version of cond-mat/0612009.

[17] Jing Yu Gan, *et al.*, Phys. Rev. B 75, 214509 (2007).

[18] G. Grynberg, *et al.*, Phys. Rev. Lett. 70, 2249 -2252 (1993).

[19] L. Santos, *et al.*, Phys. Rev. Lett. 93, 030601 (2004). B. Damski, et.al, Phys. Rev. A 72, 053612 (2005).

[20] A. Griesmaier, *et al.*, Phys. Rev. Lett. 94, 160401 (2005)

[21] K.-K. Ni, *et al.*, Science 322, 231 (2008).

[22] B. Capogrosso-Sansone, *et al.*, arXiv:0906.2009.

[23] G. Pupillo, *et al.*, arXiv:1001.0519.

[24] H. P. Bchler, *et al.*, Phys. Rev. Lett. 95, 040402 (2005).

[25] A. Chandran *et al.*, Phys. Rev. Lett. 99, 170502 (2007).

[26] Jinwu Ye, Phys. Rev. Lett. 97, 125302 (2006); Europhysics Letters, 82 (2008) 16001; J. Low Temp Phys, 160, 71 (2010).

[27] Jinwu Ye and Longhua Jiang, Phys. Rev. Lett. 98, 236802 (2007); Jinwu Ye, Phys. Rev. Lett. 97, 236803 (2006), Annals of Physics, 323, 580-630, (2008); J. Low Temp. Phys. 158, 882, (2010).